

Single-particle subband properties of quantum cables

Z.Y. Zeng^a, Y. Xiang, and L.D. Zhang

Institute of Solid State Physics, Chinese Academy of Sciences, P.O. Box 1129, Hefei, 230031, P.R. China

Received 22 March 2000 and Received in final form 6 June 2000

Abstract. We proposed a new kind of coupled coaxial cylindrical quantum wires structure – quantum cable, and calculated its single-electron energy subband spectrum for the varying structure parameters, in order to investigate its subband motion in the structure parameter space. It is shown that quantum cable has unique subband spectrum, which differs either from the (solid and hollow) cylindrical quantum wire or from the usual coupled double quantum wires (CDQWs) structure. Aside from the two-fold degeneracy induced by the cylindrical symmetry, crossings (accidental degeneracies) and anticrossings (repulsions) of quantum cable subbands with different azimuthal and radial quantum numbers are observed as one of the cable structure parameters varies. This introduces the dependence of the subband ladder on the structure parameters of the quantum cable structure. However, the subband with the lowest azimuthal and radial quantum numbers remains the lowest subband and never crosses with the other subbands irrespective of the value of structure parameters. As the coupling barrier is broadening (coupling becoming weak), some subbands bundling toward another subband is seen before the extreme isolating limit achieved. Moreover, the separation between neighboring subbands exhibits non-monotonous evolution as one changes the thickness of one of the cylindrical quantum wires, with a minimum existing in the separation between some two adjacent subbands. Interesting optical and transport phenomena arising from these unique subband properties of the quantum cable structure are also predicted.

PACS. 73.20.Dx Electron states in low-dimensional structures (superlattices, quantum well structures and multilayers) – 73.61.-r Electrical properties of specific thin films and layer structures (multilayers, superlattices, quantum wells, wires, and dots) – 03.65.Ge Solutions of wave equations: bound states

1 Introduction

Novel subband structures and unusual properties of electronic transport in low-dimensional systems have attracted current attention. It is generally believed that quantum effects become more significant as the system dimensionality is further reduced. In semiconductor, for example, confining electrons in a 2D plane, 1D wire or 0D dot gives rise to the obvious quantization of electron motion, which eventually results in some unusual transport and optical properties that are unexpected in bulk materials. With the help of these interesting properties, people can propose and fabricate nanoscale electronic devices with a variety of functions.

Since the prediction that 1D semiconductor quantum well wire (QWW) can be of importance in high-speed-device applications [1], and their subsequent fabrication [2], there has been a great deal of interest in their optical and transport properties. For QWW structures, it is a reasonable assumption that electrons are confined in a solid cylindrical quantum (SCQ) well [3], or a hollow cylindrical quantum (HCQ) well [4]. Bryant in 1984 showed that there exists an abrupt crossover

from three-dimensional to one-dimensional behavior as the SCQ wire radius is increased [3]. The transition from two-dimensional to one-dimensional behavior in HCQ wire was found by Chen *et al.* [4]. Bound states and the energy spectrum of a hydrogenic donor in QWW have been also discussed [3]. Recently, Constantinou *et al.* [5] investigated the single-electron energy subbands of the SCQ wire system in the absence and in the presence of an axial magnetic field. It is shown [5] that the subband energy given by finite confining potential is reduced compared with the values given by infinite confining potential in the absence of magnetic effect. If a magnetic field applied along the axis of the wire, a minimum in the energies associated with carriers have negative azimuthal quantum number. As to the HCQ wire structure, Masale *et al.* [6] found that, the application of an axial magnetic field leads to drastic modifications to the subband spectrum. Makar *et al.* [7] demonstrated the oscillatory behavior of the density of states for a HCQ wire under an axial magnetic field. Magneto-optical effects, collective excitation, transport behavior in cylindrical quantum wires were also actively studied [4, 8].

Coupled waveguide structures have long been the study subject of the optics and microwave community. As an analogy of coupled waveguide structures, coupled

^a e-mail: zyzeng@mail.issp.ac.cn

parallel quantum wires (CPQWs) have been extensively investigated [9]. Compared with the single quantum wire system, CPQWs possess some striking and unique features arising from the coupling between wires, such as the enhanced quantum confined Stark effect [10]. These unique features are very useful in producing numerous devices including digital switches, multiplexers, and tunable filters [11]. In 1990, coupled double quantum wires [CDQWs] device was fabricated by Alamo and Eugster [12], and its transport as well as other properties were investigated both theoretically and experimentally [13]. Recently, Suenaga *et al.* [14] and Zhang *et al.* [15] successfully synthesized a new kind of composite nanostructure termed as coaxial nanocable, in which two conducting cylindrical layers are separated by an insulating layer.

In the present work we propose a new kind of coupled quantum wire structure different from the CDQWs – quantum cable, in which two quantum wires are set to be concentric, partly stimulated by the recently fabricated coaxial nanocable structures [14,15]. Since the cylindrical quantum well is a more appropriate and convenient choice of the confining potential for electrons in quantum wires [2–4], quantum cable is chosen to be formed from two quantum cylinders, which are coupled through a controllable potential barrier. Like QWW structures, quantum cable can be also achieved from GaAlAs/GaAs system. Since for GaAlAs/GaAs system, the materials have close lattice matching. Depending on the Al concentration in $\text{Ga}_{1-x}\text{Al}_x\text{As}$, its band gap can be changed continuously, thus the shapes of the barriers and wells can be made almost to what one desires. For example, by high-resolution lithography, concentric cylindrical holes can be etched and patterned in the GaAlAs matrix. If GaAs is regrown in these holes by selective-area epitaxy, electrons would be tightly bound in the GaAs regions with cylindrical boundary [9], quantum cable is then formed. Certainly, multiple cylindrical quantum wires structure and concentric superlattice structure with cylindrical symmetry can be similarly obtained from the GaAs/AlAs systems with the help of modern etching and lithography technologies [9]. Due to the special defining potential of quantum cable structure, particular subband structure as well as optical and transport properties can be expected, which can not be anticipated in the usual CDQWs.

In the effective mass approximation, we derived the expressions for calculating the single-electron subband energy for quantum cable. We focused on the evolution of subband energy with the varied structure parameters such as cylinder thickness or the coupling barrier parameters. Numerical results demonstrated that the energy subband (0,1) remains the lowest subband either for single cylindrical quantum wires (solid and hollow) or quantum cables no matter what value of their structure parameters. Here we used the azimuthal quantum number n and the radial quantum number l to label the subband (n, l) of quantum cable system. The azimuthal quantum number n is associated with the angular momentum, while the radial quantum number l is essentially a count of the number of nodes of the radial wave function has, and is related to

the l th root of the equation (6) satisfied by the subband energy involving Bessel functions of order n . As one of the structure parameters of quantum cable is varied with others being fixed, the single-electron energy subbands associated with different azimuthal and radial quantum numbers exhibit interesting crossings (accidental degeneracies) and anticrossings (repulsions), which is the intrinsic features of the Hamiltonian system with no less than two tunable parameters [16]. However, we would like to point out that our results somewhat differ from one of the predictions by Berry, who claims that subbands with different azimuthal quantum number may cross [16]. Since the variation of the structure parameters can be regarded as a kind of perturbation to the quantum cable system, and this perturbation will be different for different subbands, thus one can observe non-monotonous variation of the separation between adjacent subbands with the varying structure parameter. Another interesting phenomenon is that a minimum exists in the non-monotonously varying separation as one changes continuously the thickness of a cylindrical quantum wire. This results in a red-shift first and then blue-shift of the optical absorption edge in the optical absorption spectrum of quantum cable structures as the thickness of a cylindrical quantum wire increases gradually. In addition, single-electron energy subbands display bundling effect as the thickness of the coupling barrier increases before the extreme isolating limit (barrier thickness tends to infinity) reached. Due to the subband crossing, subband ladder (the arrangement of subbands) is dependent on the ratio between the thicknesses of two cylindrical quantum wires. As electrons' Fermi level surpasses the energy where two subbands cross, three or four conducting channels open, depending on two subbands of what azimuthal quantum number cross. Therefore, the steps of three and four quantum conductance units ($2e^2/h$) in the ballistic electronic conductance spectrum are expected for the quantum cable structure. It is known that the width of conductance step is determined by the separation between neighboring subbands, the width of conductance step will then evolves in the similar non-monotonous way with the varied thickness of a cylindrical wire. This implies that the width of ballistic conductance step can also be adjusted, as long as one alters one of the cable structure parameters.

The paper is organized as follows. In Section 2, we derived the formulas for calculating the subband energy within the effective electron mass approximation. Section 3 presents some numerical results for the subband energy variation as a function of quantum cable structure parameters and related discussions. A brief summary is given in Section 4.

2 Model and formulation

The proposed quantum cable comprises two coaxial cylindrical quantum well wires. They are coupled through a tunable potential barrier, which allows for electron's tunneling between two cylindrical quantum wells. The defining potential of quantum cable is schematically shown in

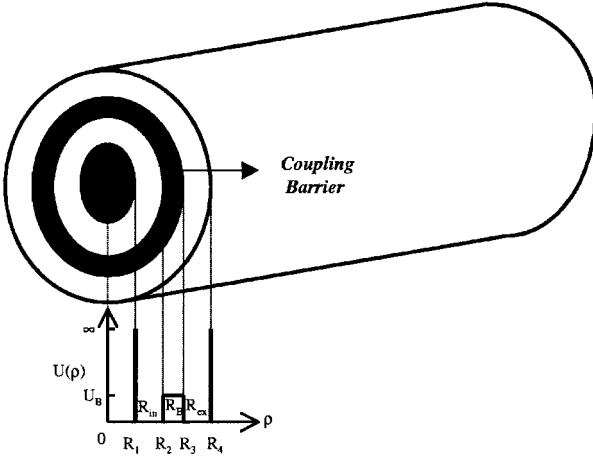


Fig. 1. Schematic view of the quantum cable structure and its defining potential profile.

Figure 1. The interior cylinder well has inner radius R_1 and outer radius R_2 , while the exterior cylinder has inner radius R_3 and outer radius R_4 . The height and thickness of the coupling barrier are U_B and $R_B = R_3 - R_2$, respectively. It can be readily shown that the thicknesses of the interior and exterior cylinders are $R_{in} = R_2 - R_1$ and $R_{ex} = R_4 - R_3$. The electrons are free to move along the longitudinal axis of quantum cable, whereas their motion in the radial direction is quantized. In the effective electron mass approximation, the Schrödinger equation governing the motion of electron with energy E reads

$$\left[-\frac{\hbar^2}{2m^*} \nabla^2 + U(\rho)\right]\Psi(\rho, \varphi, z) = E\Psi(\rho, \varphi, z), \quad (1)$$

where m^* is the effective electron mass and the defining potential of the quantum cable structure is

$$U(\rho) = \begin{cases} \infty, & \rho \leq R_1 \text{ or } \rho \geq R_4 \\ U_B, & R_2 \leq \rho \leq R_3 \\ 0, & \text{otherwise} \end{cases} \quad (2)$$

where we have adopted the hard-wall model to simulate the defining potential for simplicity. In the cylindrical coordinates (ρ, φ, z) , the wave function $\Psi(\rho, \varphi, z)$ has the form $\chi(\rho)e^{in\varphi}e^{ik_z z}$, where $n=0, \pm 1, \pm 2, \dots$, and k_z is the wavevector along the cable axis. The radial wave function $\chi(\rho)$ satisfies the following Bessel equation

$$\rho^2 \frac{d^2 \chi}{d\rho^2} + \rho \frac{d\chi}{d\rho} + \{[2m^*(E - U(\rho))/\hbar^2 - k_z^2]\rho^2 - n^2\}\chi = 0, \quad (3)$$

which has the following solutions for $E \leq U_B$

$$\chi(\rho) = \begin{cases} A_n J_n(k_1 \rho) + B_n Y_n(k_1 \rho), & R_1 \leq \rho \leq R_2 \\ C_n K_n(k_2 \rho) + D_n I_n(k_2 \rho), & R_2 \leq \rho \leq R_3 \\ F_n J_n(k_1 \rho) + G_n Y_n(k_1 \rho), & R_3 \leq \rho \leq R_4 \\ 0, & \rho \leq R_1 \text{ or } \rho \geq R_4 \end{cases} \quad (4)$$

where J_n is the Bessel function of the first kind, Y_n the Bessel function of the second kind, K_n, I_n are the modified Bessel functions [17], and

$$k_1 = [(2m_1^*/\hbar^2)E - k_z^2]^{1/2}, \\ k_2 = [(2m_2^*/\hbar^2)(U_B - E) + k_z^2]^{1/2}, (E \leq U_B), \quad (5)$$

are the wavevectors with m_i^* ($i = 1, 2$) being the effective electron mass in medium i . We now apply the standard effective-mass boundary conditions at $\rho = R_1, R_2, R_3, R_4$, which lead to the following transcendental equation satisfied by the subband energy:

$$\frac{k_2}{m_2^*} f_1(k_1; R_1, R_2) \left[\frac{k_2}{m_2^*} F_1(k_1, k_2; R_2, R_3, R_4) \right. \\ \left. + \frac{k_1}{m_1^*} F_2(k_1, k_2; R_2, R_3, R_4) \right] + \frac{k_1}{m_1^*} g_1(k_1; R_1, R_2) \\ \times \left[\frac{k_2}{m_2^*} G_1(k_1, k_2; R_2, R_3, R_4) + \frac{k_1}{m_1^*} G_2(k_1, k_2; R_2, R_3, R_4) \right] \\ = 0, \quad (6)$$

where

$$f_1(k_1; R_1, R_2) = J_n(k_1 R_2) Y_n(k_1 R_1) \\ - J_n(k_1 R_1) Y_n(k_1 R_2), \\ g_1(k_1; R_1, R_2) = J_n(k_1 R_1) Y_n'(k_1 R_2) \\ - J_n'(k_1 R_2) Y_n(k_1 R_1), \\ F_1(k_1, k_2; R_2, R_3, R_4) = [K_n'(k_2 R_3) I_n'(k_2 R_2) \\ - K_n'(k_2 R_2) I_n'(k_2 R_3)] \\ \times [J_n(k_1 R_4) Y_n(k_1 R_3) \\ - J_n(k_1 R_3) Y_n(k_1 R_4)], \\ F_2(k_1, k_2; R_2, R_3, R_4) = [K_n(k_2 R_3) I_n'(k_2 R_2) \\ - K_n'(k_2 R_2) I_n(k_2 R_3)] \\ \times [J_n'(k_1 R_3) Y_n(k_1 R_4) \\ - J_n(k_1 R_4) Y_n'(k_1 R_3)], \\ G_1(k_1, k_2; R_2, R_3, R_4) = [K_n'(k_2 R_3) I_n(k_2 R_2) \\ - K_n(k_2 R_2) I_n'(k_2 R_3)] \\ \times [J_n(k_1 R_4) Y_n(k_1 R_3) \\ - J_n(k_1 R_3) Y_n(k_1 R_4)], \\ G_2(k_1, k_2; R_2, R_3, R_4) = [K_n(k_2 R_3) I_n(k_2 R_2) \\ - K_n(k_2 R_2) I_n(k_2 R_3)] \\ \times [J_n'(k_1 R_3) Y_n(k_1 R_4) \\ - J_n(k_1 R_4) Y_n'(k_1 R_3)], \quad (7)$$

where $f'(x) = df(x)/dx$. Equation (6) may be solved numerically by employing the recursion relations satisfied by the Bessel functions [17]. With the help of the properties and recursion relations of the Bessel functions [17], one can readily prove that $E_{nl} = E_{-nl}$, *i.e.*, the subbands with azimuthal quantum number n and $-n$ are degenerate. The two-fold degeneration of energy subbands of quantum cable with nonzero azimuthal quantum number originates from

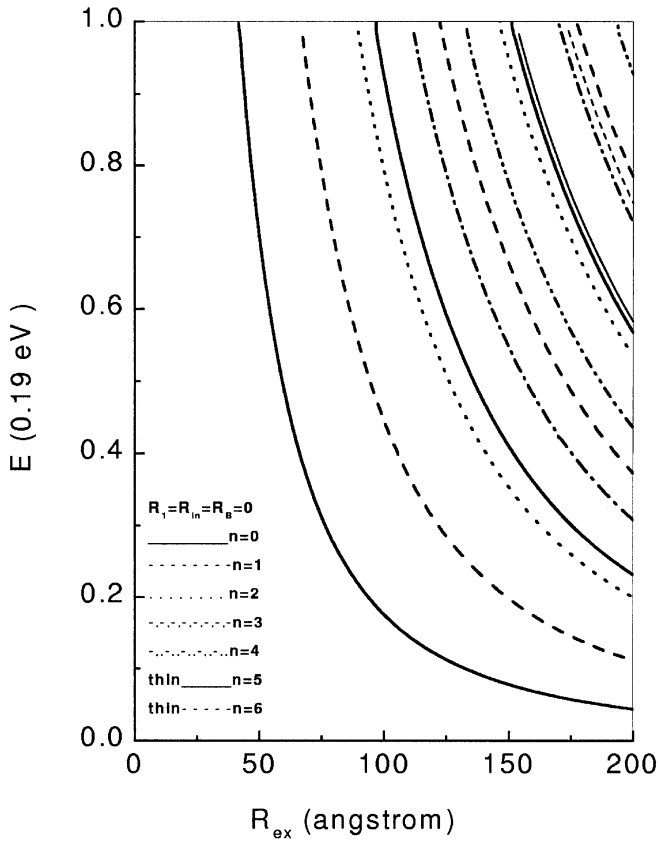


Fig. 2. Lowest-order subband energy of solid cylindrical quantum wires as a function of its radius.

the cylindrical symmetry of the cable defining potential. It is noted that the scheme for calculating the subband energy is exact within the effective mass model used.

3 Results and discussions

To start with, we study the subband spectrum of single cylindrical quantum wires. As stated in the introduction, we can visualize the quantum cylinders and quantum cable as GaAs wire (wires) surrounded by $\text{Ga}_{0.7}\text{Al}_{0.3}\text{As}$ layer(layers), for which the parameters are $m_1^* = 0.067m_e$, $m_2^* = 1.4m_1^*$. The barrier height is set as $U_B = 0.19$ eV for the convenience of comparison with the results of references [5] and [6]. Figure 2 gives the relation of subband energy with the SCQ wire radius $R = R_{\text{ex}}$ (where $R_1 = R_{\text{in}} = R_B = 0$). The subband energy E_{nl} is related to the total energy via $E = E_{nl} + \hbar^2 k_z^2 / (2m^*)$, and is labeled by the azimuthal quantum number n and the radial quantum number l . For simplicity, we take $k_z = 0$ in the calculations throughout this paper. As expected, the subband energy as well as the energy difference between adjacent subbands decreases with the increasing wire radius R_{ex} , and the separation between adjoining lower-order subbands is greater than that between higher-order ones. The subbands are arranged such that (0,1), (1,1), (2,1), (0,2)... and this subband ladder remains unchanged no matter what value of the solid cylinder radius.

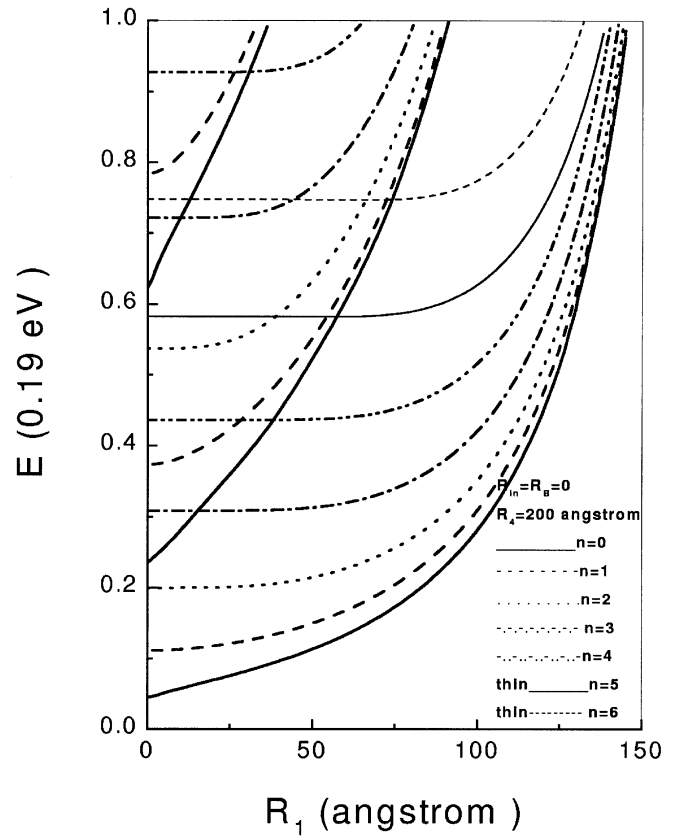


Fig. 3. Lowest-order subband energy of hollow cylindrical quantum wires as a function of its inner radius.

It is clear that for a given n , the value of R at which a confined subband appears satisfies $J_n(k_1 R) = 0$, which can be also derived from the equations (6, 7) by employing the properties and recursion relations of Bessel functions [17]. In Figure 3 we present the calculated results for subband energy of a HCQ wire versus its inner radius R_1 with a given outer radius $R_4 = 200$ Å (where we choose $R_{\text{in}} = R_B = 0$). It is seen that the subbands with equal radial quantum number l converge as the width $R_4 - R_1$ of the HCQ wire approaches zero, with their energies having a $(R_4 - R_1)^{-2}$ variation. As the inner radius R_1 tends to zero while the outer radius R_4 keeps unchanged, one can observe an appreciable separation between the subbands corresponding to different n but equal l . These features can also be understood from the properties of Bessel functions. At the same time, crossings (accidental degeneracies) involving two high-order subbands with different azimuthal and radial quantum numbers $\{n, l\}$ are also observed as the inner or outer radius of the HCQ wire is varied. However, the subband (0,1) remains the lowest subband either in SCQ wire case or in HCQ wire case, which is independent of the structure parameters. The subband crossings (accidental degeneracies) are different from the normal two-fold degeneracies of energy subbands which arises from the cylindrical symmetry. It originates neither from some kind of hidden symmetry nor from dynamic effect, in view of Berry's argument [16]. We suggest that it is an intrinsic characteristic of the real Hamiltonian

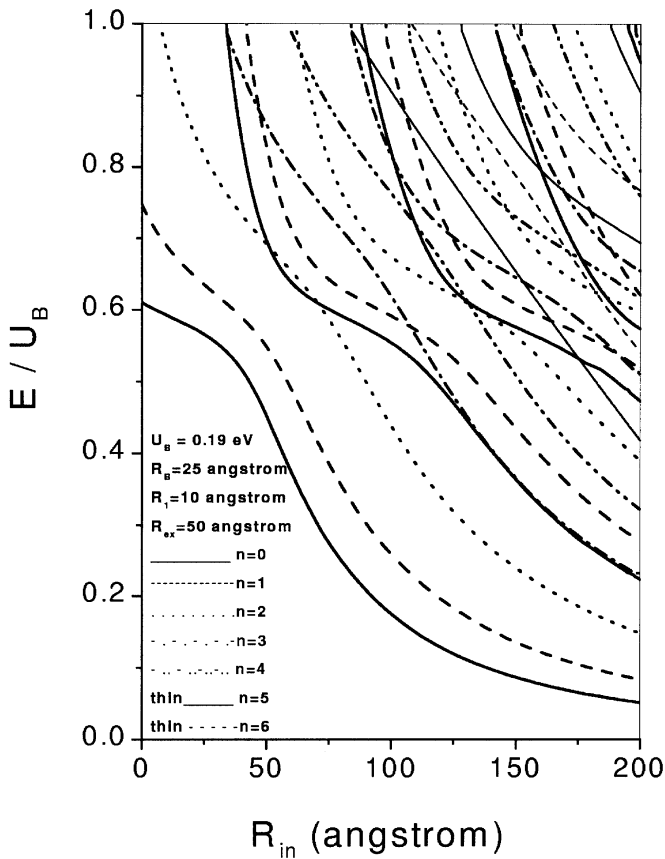


Fig. 4. Lowest-order subband energy of the quantum cable with two hollow cylinders as a function of its interior wire thickness R_{in} .

system involving no less than two variable geometric parameters, since no subband crossing is seen in SCQ wires which has only one parameter -its radius R . As early as in 1929, von Neumann and Wigner [18] proposed that for real Hamiltonian systems, one parameter is in general insufficient to produce a degeneracy, at least two are required. Later Berry predicted that level crossings would occur in a two-dimensional potential involving two parameters with circular symmetry, and he called such level crossings “diabolical points” in the energy-level surface [16]. Obviously, subband crossings would also be observed in the subband spectrum of quantum cable with more variable parameters, as we will show later. Comparing our results with that in references [5,6], one will find that our results obtained from equation (6) is in very good agreement with Constantinou group’s [5,6], which demonstrated the reliability of our formulation.

Now we inspect the energy subband structure of the first kind of quantum cable, which comprises coupled two HCQ wires. The variation of subband energy with the interior cylinder thickness R_{in} is given in Figure 4 and that with the exterior cylinder thickness R_{ex} in Figure 5. The parameters are chosen such that $U_B = 0.19$ eV, $R_B = 25$ Å, $R_1 = 10$ Å. Energy subbands of quantum cable are also denoted by the azimuthal quantum number n and the radial quantum number l . In Figures 4 and 5, we noticed that the subband (0, 1) is also the lowest subband

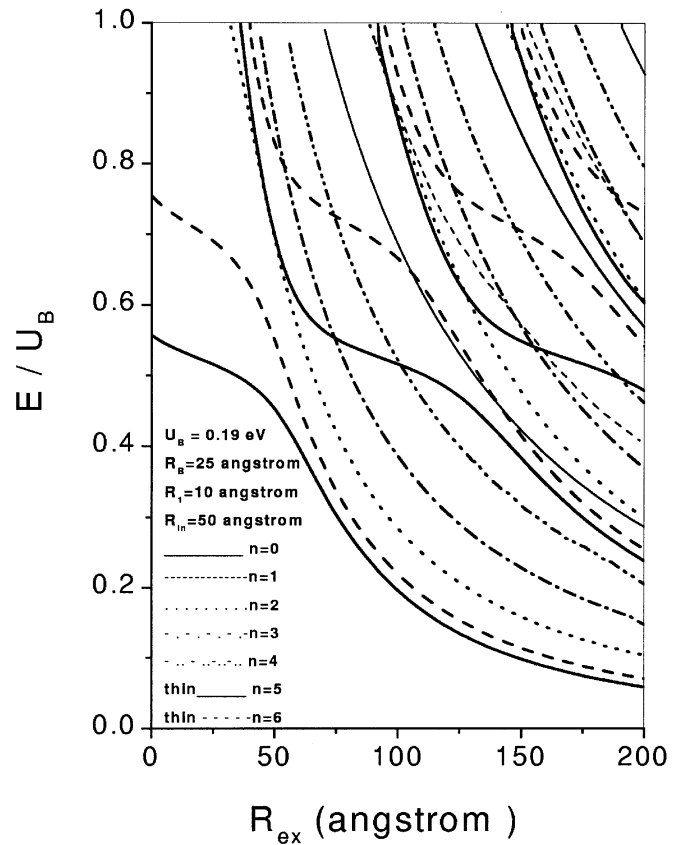


Fig. 5. Lowest-order subband energy of quantum cable with two hollow cylinders as a function of its exterior wire thickness R_{ex} .

and never crosses with other subbands for the first kind of quantum cable. Since two cylindrical quantum wires are coupled through a barrier, more complicated and interesting subband energy evolution with the varying structure parameters can be expected. Having check the quantum numbers of the crossing subbands, we find that, crossings are only seen for two subbands belonging to different azimuthal and radial quantum numbers, and never occur for the subbands with the same azimuthal quantum number or the same radial quantum number. This result differs to some extent from the prediction of Berry which suggests that subbands with different azimuthal quantum numbers may cross [16]. Whereas for subbands with the same azimuthal quantum number, they may exhibit anticrossings (repulsions) within some parameter (R_{in} or R_{ex}) regions. As the thickness (R_{in} or R_{ex}) increases, the separation between some two adjacent subbands evolves non-monotonously. By calculating the non-monotonously varied separation, we noticed that there exists a minimum in such separation. The minimum separation between neighboring subbands with larger quantum numbers corresponds to larger cylinder thickness R_{in} or R_{ex} . Based on the same argument on subband crossings for the HCQ wire structure, crossings and anticrossings are not induced by some kind of hidden geometric symmetry. It is also the intrinsic property of the Hamiltonian system of no less than two variable structure parameters, which will

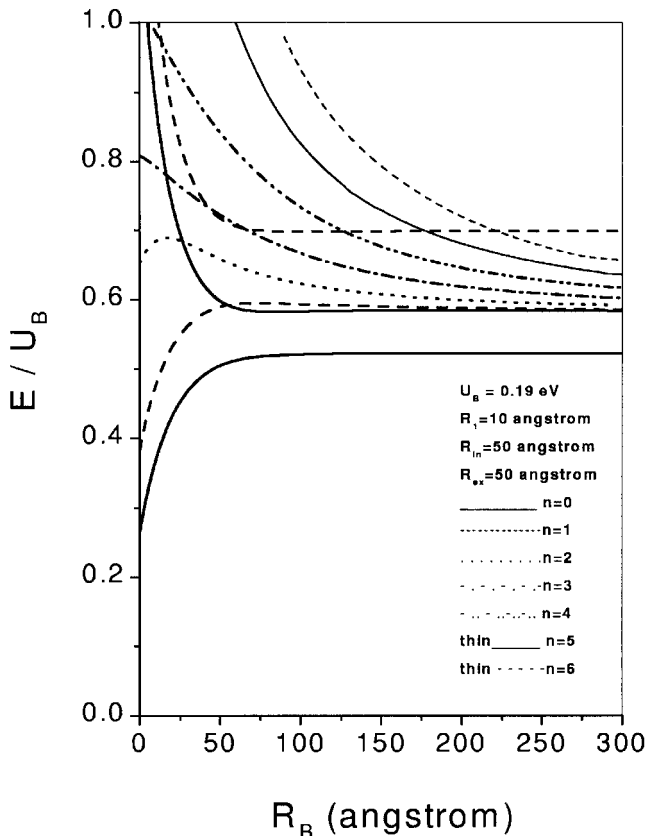


Fig. 6. Lowest-order subband energy of quantum cable with two hollow cylinders as a function of the coupling barrier thickness R_B .

be confirmed by the subband energy variation as a function of the coupling strength parameter (barrier thickness or height). From the physical point of view, subband crossings and anticrossings as well as the non-monotonous variation of the subband separations are due to the fact that, varying the thickness of one cylindrical quantum wire can be regarded as a perturbation to the system, which causes different energy shifts for different subbands; or in other words, such perturbation introduces re-distribution of electron wavepacket between two cylindrical wires [13]. In view of the subband crossings, one can not determine the subband ladder of the quantum cable structure simply from subband's azimuthal and radial quantum numbers without knowing the related cable structure parameters.

In Figure 6, we give the energy variation of low-lying subbands with the increasing barrier thickness R_B . Other parameters are set as $R_1 = 10 \text{ \AA}$, $R_{in} = R_{ex} = 50 \text{ \AA}$ and $U_B = 0.19 \text{ eV}$. One can readily find that, as the barrier thickness increases, the energy of subbands (0, 1) and (1, 1) rises first and then varies slowly, until the extreme isolating limit $R_B \rightarrow \infty$ is reached, then it remains unchanged. While for subbands (0, 2) and (1, 2), their energy drops first and then varies smoothly. This reflects the fact that the coupling of two cylindrical wells becomes weak for large R_B . There is another interesting phenomenon to be worth mentioning, *i.e.*, the energy of the subband (2, 1) increases first, over a critical R_B , it decreases monotonically

and then changes slowly before the extreme isolating limit arrived. Subband crossings can be also observed in the case of varying coupling strength (barrier thickness or height [19]), which suggests that subband crossings and anticrossings are not a kind of dynamic effect. It is also originated from the multi-variable-parameter properties of the real Hamiltonian of quantum cable structure. As the barrier thickness increases, we observed another significant phenomenon that some high-lying subbands bundle toward the subband (0, 2) before the coupling barrier thickness tends to infinity. In the extreme isolating case, the subband dispersions for the decoupled quantum cable structure will be the simple superposition of the subband dispersions of individual cylindrical wires. As in other cases, for increasing barrier thickness, the lowest subband is also related to that with the lowest azimuthal and radial quantum numbers (0, 1). If the radius of the infinite potential barrier core is zero, quantum cable turns into the coupled SCQ wire and HCQ wire structure. It is expected that similar subband spectrum and subband motion in the structure parameter space do hold for this kind of quantum cable structure [20].

So far, we investigated the energy subband motion in the parameter space of the quantum cable structure. Comparing the subband spectrum of quantum cable with that of the symmetric CDQWS (here the word 'symmetric' implies the two quantum waveguides have the same widths), we find there are some significant discrepancies between them. As the width of the coupling barrier increases, the subbands with the same symmetry will be degenerated for the CDQWs structure, while this does not hold for the quantum cable of two quantum cylinders with the same thickness. On the other hand, if two quantum wells of CDQWs have different widths, it is impossible to find that two subbands will be degenerated (normally or accidentally) as the coupling becomes weak, since in this case the confining potential and thus electron wavefunctions have no particular symmetry. Moreover, a minimum can not be expected in the separation between adjacent subbands of CDQWs as a wire width varies. It is appropriate for us to discuss roughly the possible optical and transport phenomena associated with the particular subband behaviors of quantum cable. First, subband crossings may induce the stronger optical absorption, and ballistic conductance steps of more than two quanta for quantum cable. This can be easily understood, as the subband crossing occurs, quantum cable system will provide doubled conducting channels or available transition states. Second, as the thickness of one cylindrical wire of quantum cable increases, one may observe a red-shift first and then blue-shift of the optical absorption edge in the optical absorption spectrum of quantum cable structures, and the alternative squeezing and broadening of ballistic conductance plateaus, due to the non-monotonous variation of the separation between neighboring subbands with the varying parameter. These unique features may be employed in some quantum devices. Using the subband bundling effects in the case of increasing barrier thickness, people can adjust optical and ballistic transport spectrum

in a favorable manner. If quantum cable is extended to the multiple coaxial cylindrical quantum wire structure, crossings involving more subbands would be anticipated. At the same time, we believe that the unusual subband structure can also be expected in the coupled concentric quantum dot systems. We hope that the predicted optical and transport phenomena would be observed in the near future. Based on the above analysis, we believe that quantum cable is one of the promising candidates for the future mesoscopic devices.

4 Conclusions

In summary, we proposed a new kind of coupled coaxial quantum wire structure – quantum cable – which consists of two coaxial cylindrical quantum wires coupled through a tunable potential barrier. In the effective mass approximation, we derived the expressions for calculating the subband energy of quantum cable. As a function of cable structure parameters such as wire thickness and barrier thickness, the single-electron subbands of quantum cable exhibit some interesting and unique behaviors unexpected in other nanostructures. The significant phenomena observed in quantum cable systems include crossings and anticrossings for the subbands with different azimuthal and radial quantum numbers, non-monotonous variation of the separation between some neighboring subbands and the subband bundling in the case of widening barrier thickness. The results obtained in this paper suggest that quantum cable is a good candidate for the study of subband motion in the structure parameter space for the Hamiltonian system with more than two variable parameters. We also discussed the possible optical and transport effects associated with the peculiar subband properties of quantum cables.

This work is supported by a key project for fundamental research in the National Climbing Program of China. We would also like to acknowledge the valuable suggestions of the referees.

References

1. H. Sakaki, *Jpn J. Appl. Phys.* **19**, L735 (1980).
2. P.M. Petroff, A.C. Gossard, R.A. Logan, W. Wiegmann, *Appl. Phys. Lett.* **41**, 635 (1982); T.J. Thornton, M. Pepper, H. Ahmed, D. Andrews, G.J. Davies, *Phys. Rev. Lett.* **56**, 1198 (1986); J. Cibert, P.M. Petroff, G.J. Dplan, S.J. Pearton, A.C. Gossard, J.H. English, *Appl. Phys. Lett.* **49**, 1275 (1986); H. Temkin, G.J. Doaln, M.B. Parish, S. N.G. Chu, *ibid.* **50**, 413 (1987).
3. G.W. Bryant, *Phys. Rev. B* **29**, 6632 (1984).
4. H. Chen, Y. Zhu, S. Zhou, *Phys. Rev. B* **36**, 8189 (1987).
5. N.C. Constantinou, B.K. Ridley, *J. Phys. Cond. Matt.* **1**, 2283 (1989); N.C. Constantinou, M. Massale, D.R. Tilley, *ibid.* **4**, 4499 (1992).
6. M. Massale, N.C. Constantinou, D.R. Tilley, *Phys. Rev. B* **46**, 15432 (1992).
7. M.N. Makar, M.A. Ahmed, M.S. Awad, *Phys. Stat. Sol. (b)* **167**, 647 (1991).
8. T. Kamizato, M. Matsuura, *Phys. Rev. B* **40**, 8378 (1989); F.Y. Huang, *ibid.* **41**, 12957 (1990); L. Wendler, V.G. Grigoryan, *ibid.* **49**, 14531 (1994); E.P. Pokatilov, S.N. Klimin, S.N. Balaban, V.M. Fomin, *Phys. Stat. Sol. (b)* **189**, 433 (1995).
9. M.A. Morrison, T.L. Estle, N.F. Lane, *Quantum States of Atoms, Molecules, and Solids* (Prentice-Hall Inc. 1976); D. Sarma, D.K. Lai, *Phys. Rev. B* **32**, 1401 (1985); G.J. Iafrate, D.K. Ferry, R.K. Reich, *Surf. Sci.* **113**, 485 (1981); W. Que, S.E. Kirczenow *Phys. Rev. B* **37**, 7153 (1988); T.V. Shahbazyan, S.E. Ulloa, *ibid.* **54**, 16749 (1996).
10. H. Kroemer, D. Okamoto, *Jpn J. Appl. Phys.* **23**, 970 (1984).
11. A. Yariv, *Optical Electronics* (HRW, New York, 1985).
12. J.A. del Alamo, C.C. Eugster, *Appl. Phys. Lett.* **56**, 76 (1990).
13. R.Q. Yang, J.M. Xu, *Phys. Rev. B* **43**, 1699 (1991); P. Zhao, *ibid.* **45**, 4301 (1992); G. Xu, M. Yang, P. Jiang, *J. Appl. Phys.* **74**, 6747 (1993); C.C. Eugster, J.A. del Alamo, M.J. Rooks, M.R. Melloch, *Appl. Phys. Lett.* **60**, 642 (1992); C.C. Eugster, J.A. del Alamo, M.R. Melloch, M.J. Rooks, *Phys. Rev. B* **46**, 10406 (1992); **48**, 15057 (1993); J. Wang, H. Guo, R. Harris, *Appl. Phys. Lett.* **59**, 3075 (1991); J. Wang, Y.J. Wang, R. Harris, *Phys. Rev. B* **46**, 2420 (1992); J.R. Shi, B.Y. Gu, *ibid.* **55**, 9941 (1997).
14. K. Suenaga, C. Colliex, N. Demoncy, A. Loiseau, H. Pascard, F. Willaime, *Science* **278**, 653 (1997).
15. Y. Zhang, K. Suenaga, C. Colliex, S. Iijima, *Science* **281**, 973 (1998).
16. M.V. Berry, M. Wilkinson, *Proc. R. Soc. Lond. A* **392**, 15 (1984); M.V. Berry, *ibid.* **392**, 45 (1984).
17. *Handbook of Mathematical Functions* edited by M. Abramowitz, I.A. Stegun (Dover, New York, 1972).
18. E.P. Wigner, J. von Neumann, *J. Phys. Zeif.* **30**, 467 (1929).
19. We also studied the variation of subband energy of quantum cable as a function of the coupling barrier height, finding that subband crossings also exist in this case. This urges us to believe that the subband crossings originate neither from hidden symmetry nor dynamic effect.
20. Z.Y. Zeng *et al.* (unpublished).